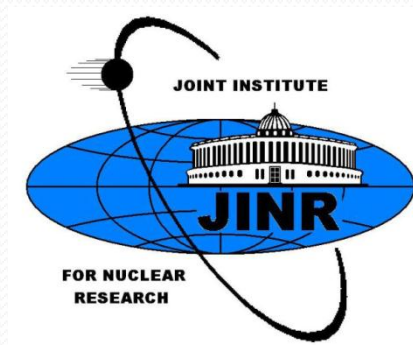
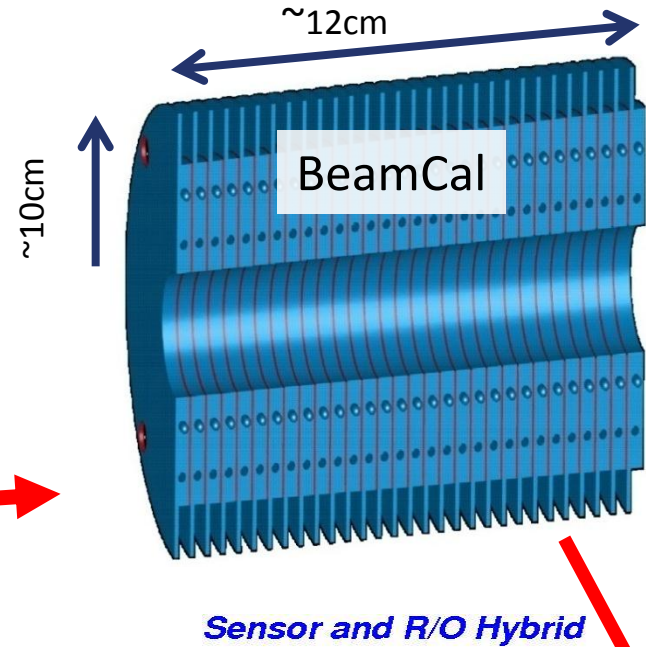
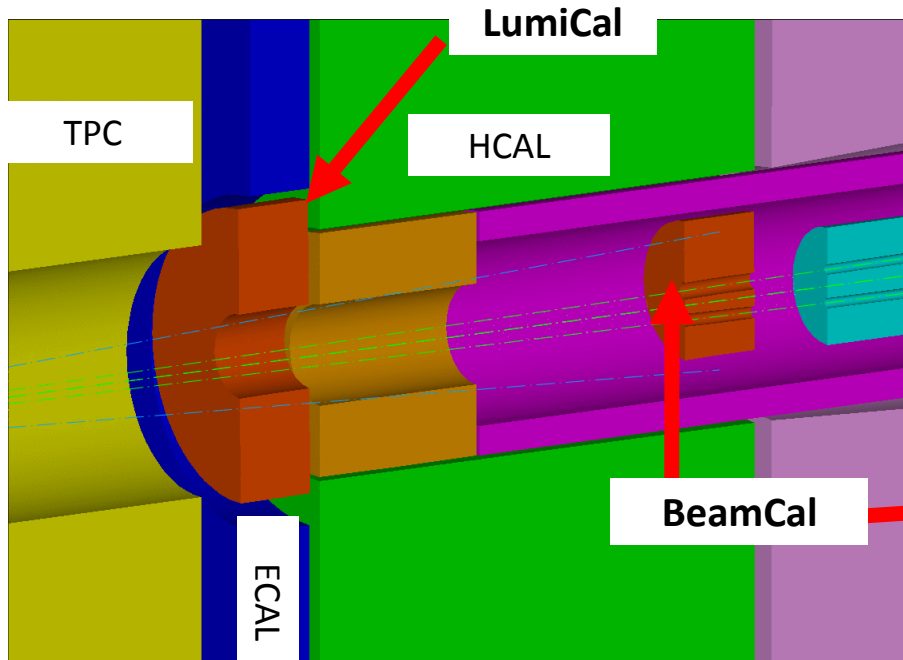


Results of measuring GaAs sensor planes

U.Kruchonak, V. Elkin, O.Novgorodova



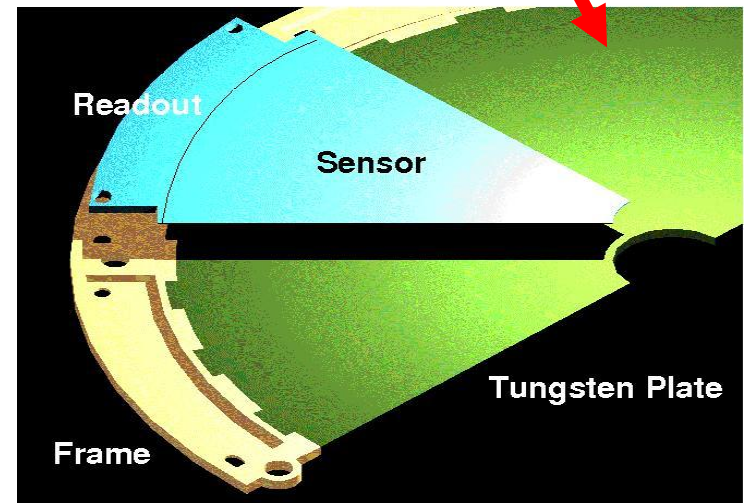
The Beam Calorimeter - BeamCal



Compact EM calorimeter with sandwich structure:

- ❖ 30 layers of $1 X_0$
o 3.5mm W absorber and 0.3mm radiation hard sensor
- ❖ Angular coverage from 5mrad to 28 mrad
($6.0 > |\eta| > 4.3$)
- ❖ Molière radius $R_M \approx 1\text{cm}$
- ❖ Segmentation between 0.5 and $0.8 \times R_M$

GaAs:Cr is offered as a radiation hard sensor for Beamcal.



The main characteristics of semiconductor materials

Material	Density, g/cm ⁻³	Atomic number	Band gap, eV	$\mu\tau$ product , cm ² /V	
				$\mu_n \tau_n$	$\mu_p \tau_p$
Si	2.33	14	1.12	~ 1	~ 1
GaAs	5.32	~ 32	1.43	~ 10 ⁻⁴	~ 10 ⁻⁵
CdTe	5.85	~ 49	1.5	10 ⁻³	10 ⁻⁴
Hgl ₂	6.4	~ 81	2.13	10 ⁻⁴	10 ⁻⁵
Pbl ₂	6.16	~ 83	2.32	10 ⁻⁵	10 ⁻⁶

We can see that the pure (not doped) Si has the charge carriers lifetime which exceeds the lifetime for binary semiconductors by 4 orders. **However, pure semiconductors (Si) have not sufficient radiation hardness and relatively small conversion efficiency for γ .**

GaAs:Cr Sensor Plane

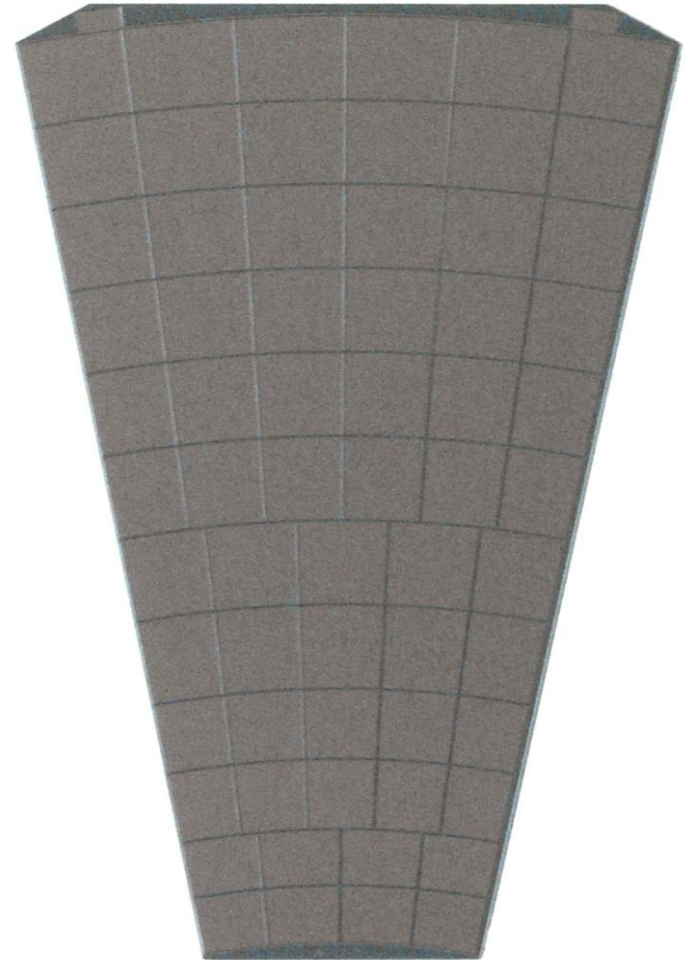
- Produced by the Siberian Institute of Technology, Tomsk
- semi-insulating GaAs doped by Sn (shallow donor)
- compensated by Cr (deep acceptor): to compensate electron trapping centers EL2+ and provide i-type conductivity.
- Due to a wider band gap these samples are radiation harder and have a lower leakage current (resistivity $>10^9$ Ohm*sm)

BUT....

- Due to small holes mobility only electron charge can be collected. It limits maximum CCE to 50% for minimum ionising particles.

GaAs:Cr Sensor Plane

- **New set of 11 sector size GaAs sensors (22 at all)**
- **Thickness - 500 μm**
- **Metallization $\sim 1 \mu\text{m}$ Ni both sides**
- **12 rings**
- **64 pads from 18 to 42 mm^2**
- **Surrounded by 120 μm width guard ring**



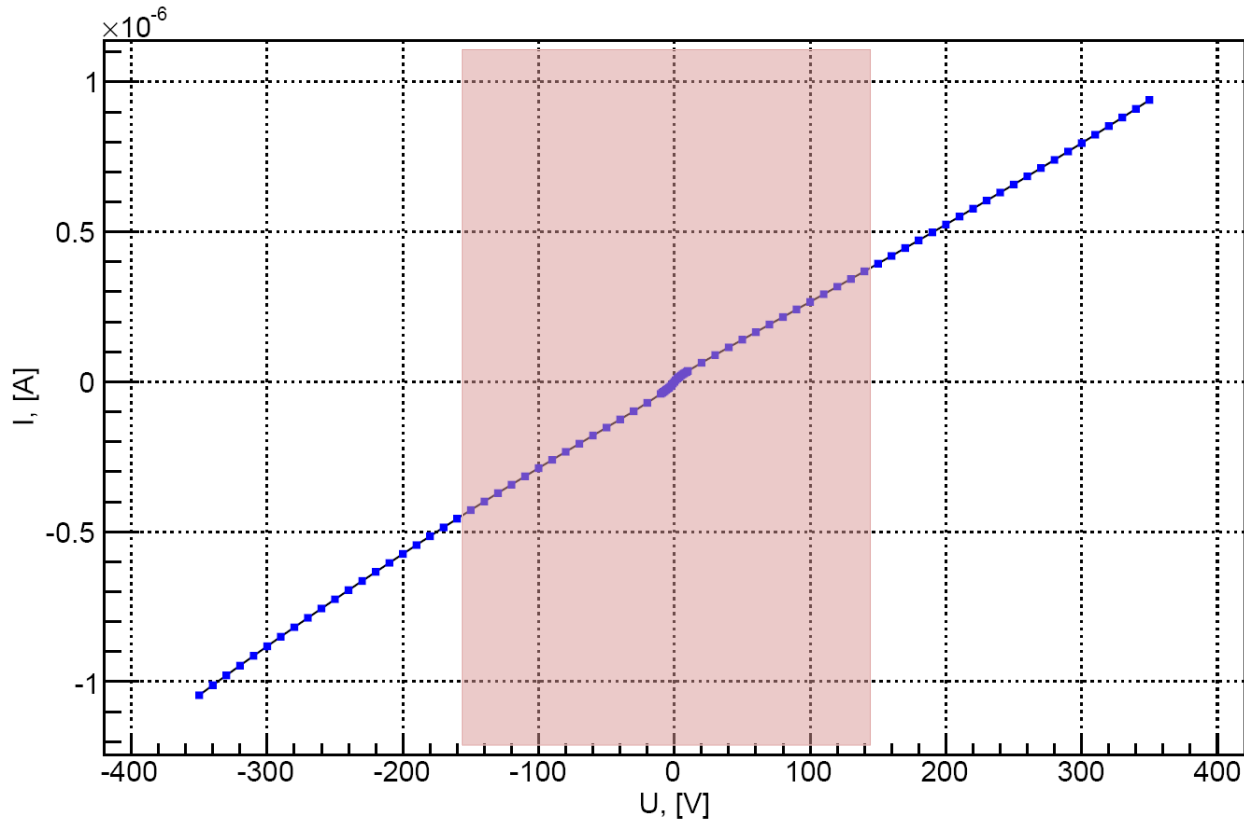
GaAs:Cr Sensor producer data

№	Detector	thickness, um	collected charge, e*	metallization, Type of metallization	
				pixels	Guard ring
1	AG-262 №1	506	40570	Ni	Ni
2	AG-262 №3	512	41640	Ni	Ni
3	AG-262 №4	509	42690	Ni	Ni
4	AG-221 №6	498	37020	Ni	Ni
5	AG-262 №12	504	35630	Ni	Ni
6	AG-262 №13	517	37580	Ni	Ni
7	AG-262 №15	518	39190	Ni	Ni
8	AG-262 №16	509	37170	Ni	Ni
9	AG-262 №19	507	34490	Ni	Ni
10	AG 84 № 23	492	37930	Ni	Ni
11	AG 84 №24	485	38520	Ni	Ni

* - $U_{\text{bias}} = -150\text{V}$, RT, β - radiation (^{90}Sr , mip).

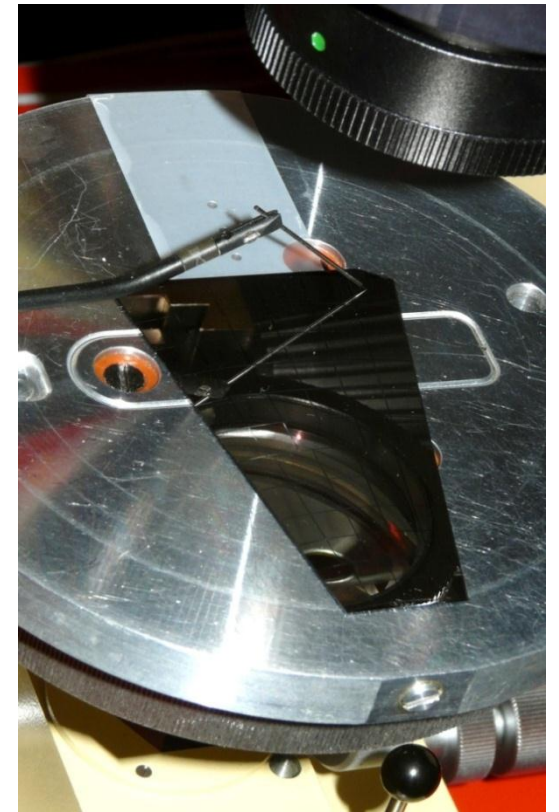
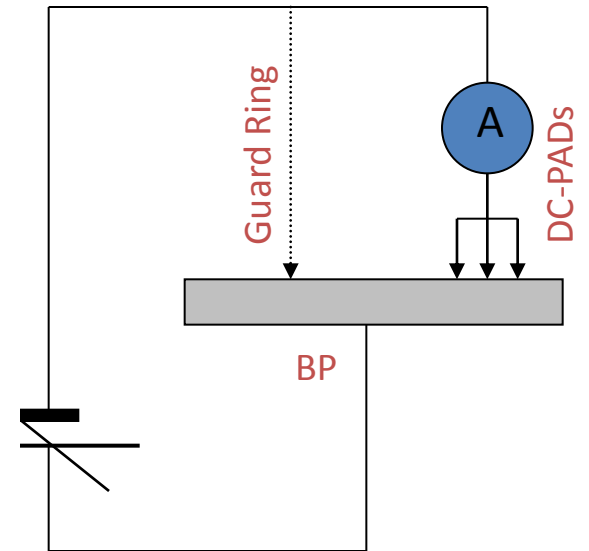
I/V pad measurements

IV characteristic R11P05

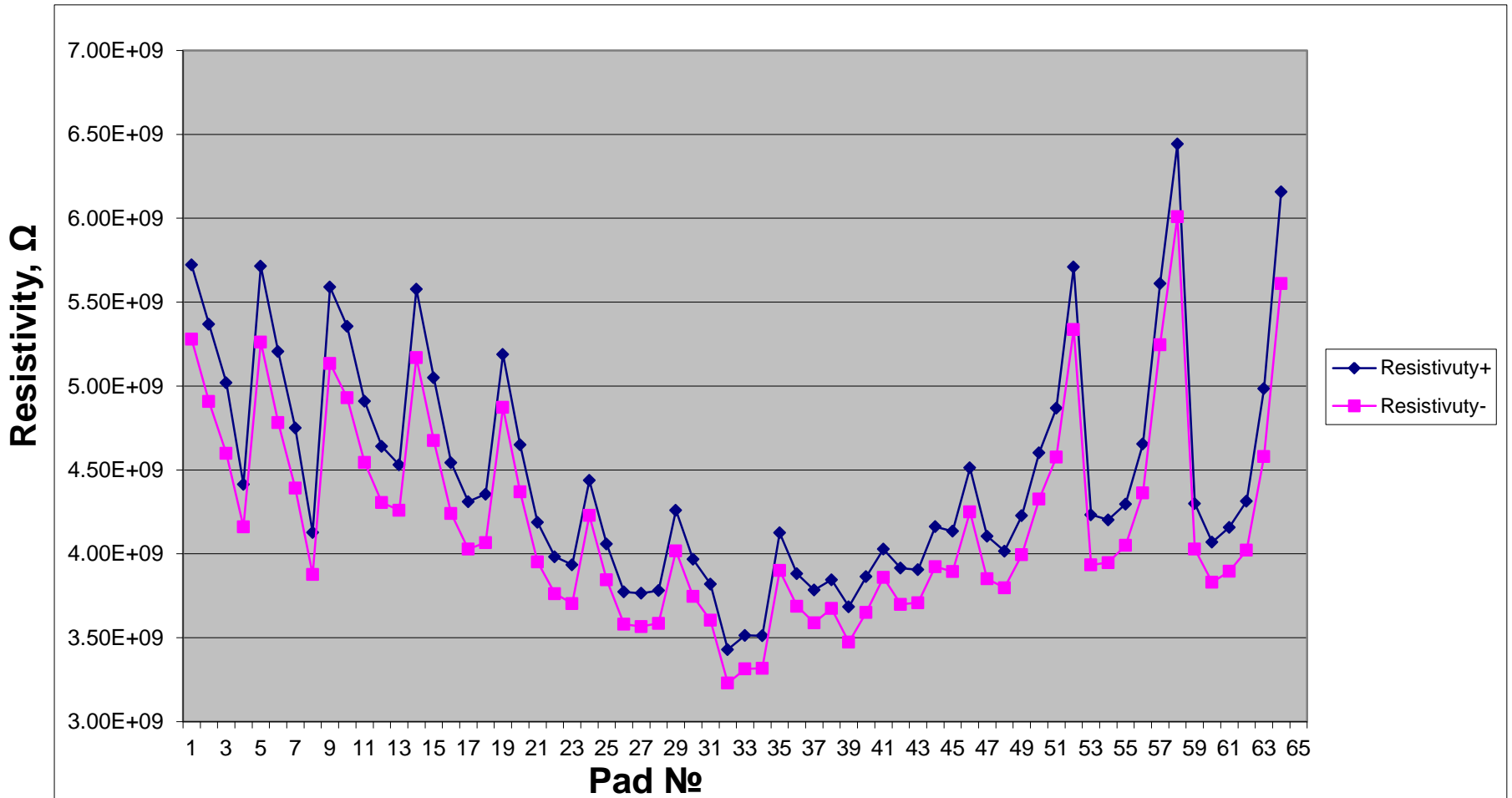


Typical IV of one pad of AG-262N \circ 3

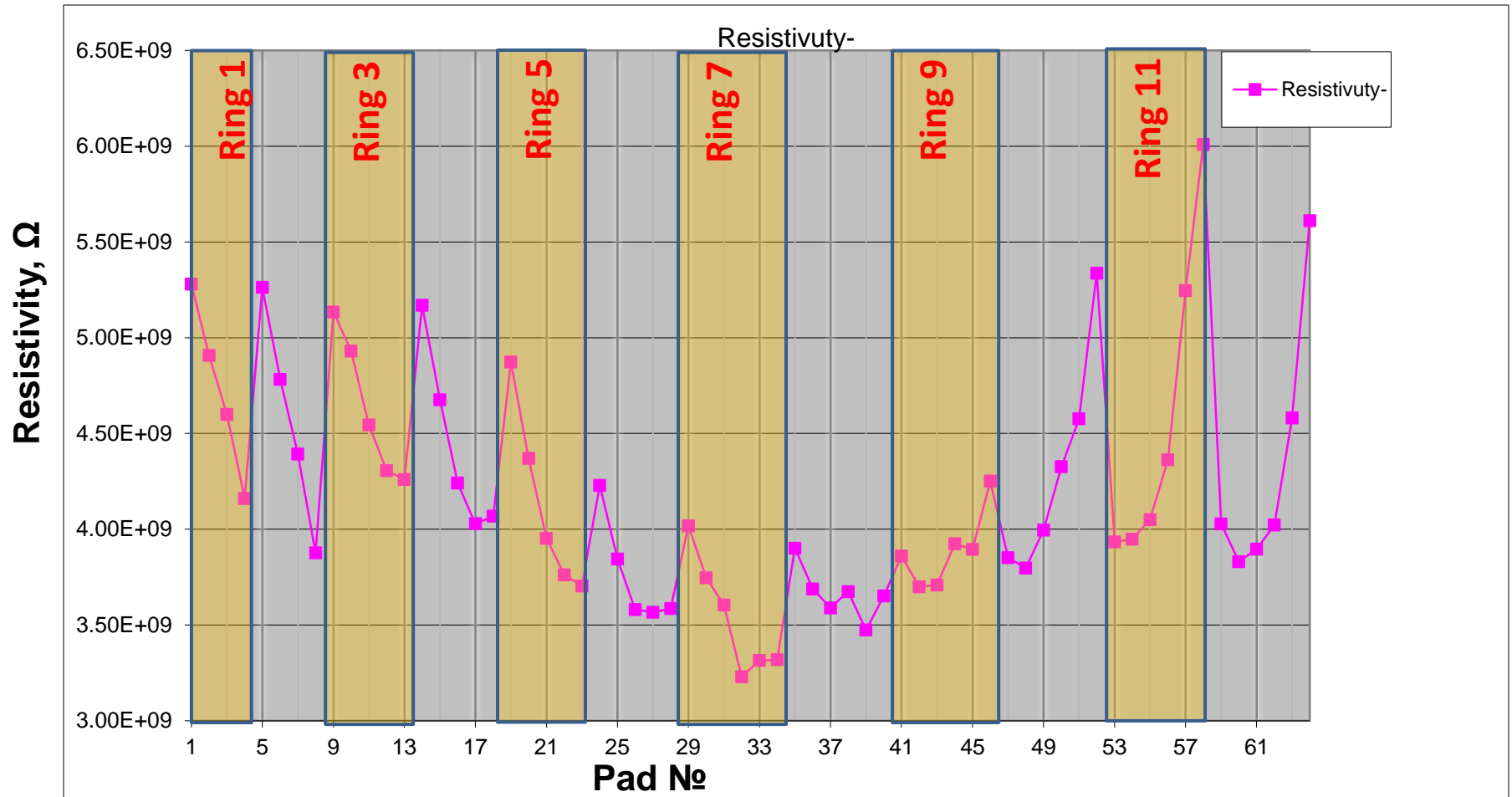
- symmetric in the range $\pm 350\text{V}$
- linear in the range $\pm 150\text{V}$



Resistivity pads distribution of AG221№6



Resistivity pads distribution of AG221№6



It was found that for some sensors the ρ^- , ρ^+ strongly depends on Ring №

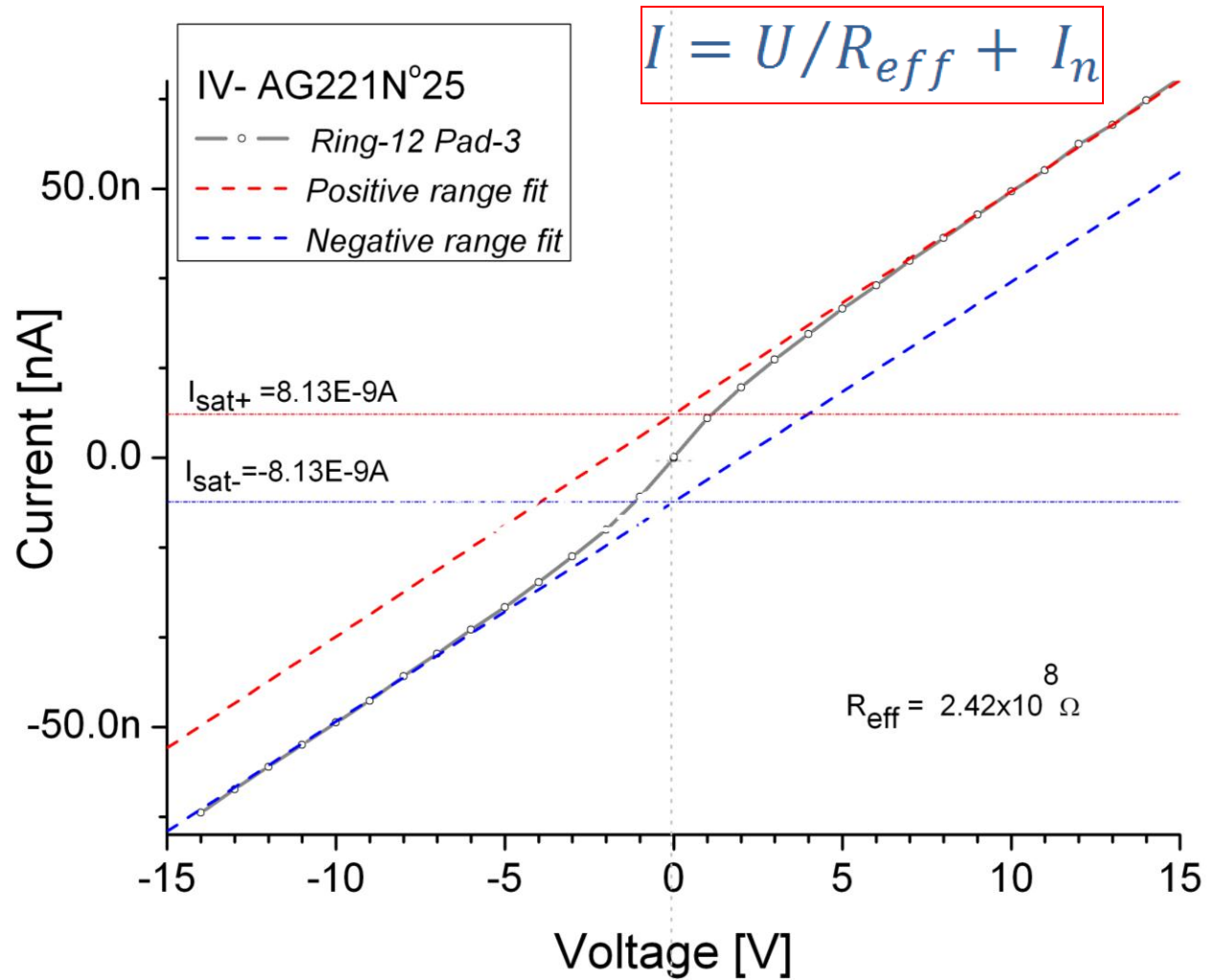
I-V in range +/-10V

Parameterization of the IV curve by 4 parameters:

- I_{n-}
- I_{n+}
- R_{-}
- R_{+}

As result of IV measurement we can get 4 parameters for each pad:

ρ_{-} , ρ_{+}
 φ_{-} , φ_{+}



Measurement of the barrier height on border of metal–*semiinsulating* gallium arsenide

total current through the device

$$I = U/R_{eff} + I_n$$

R_{eff} - effective resistance of the entire device

I_n or I_{sat} - Saturation current - Limiting current from metal to semiconductor

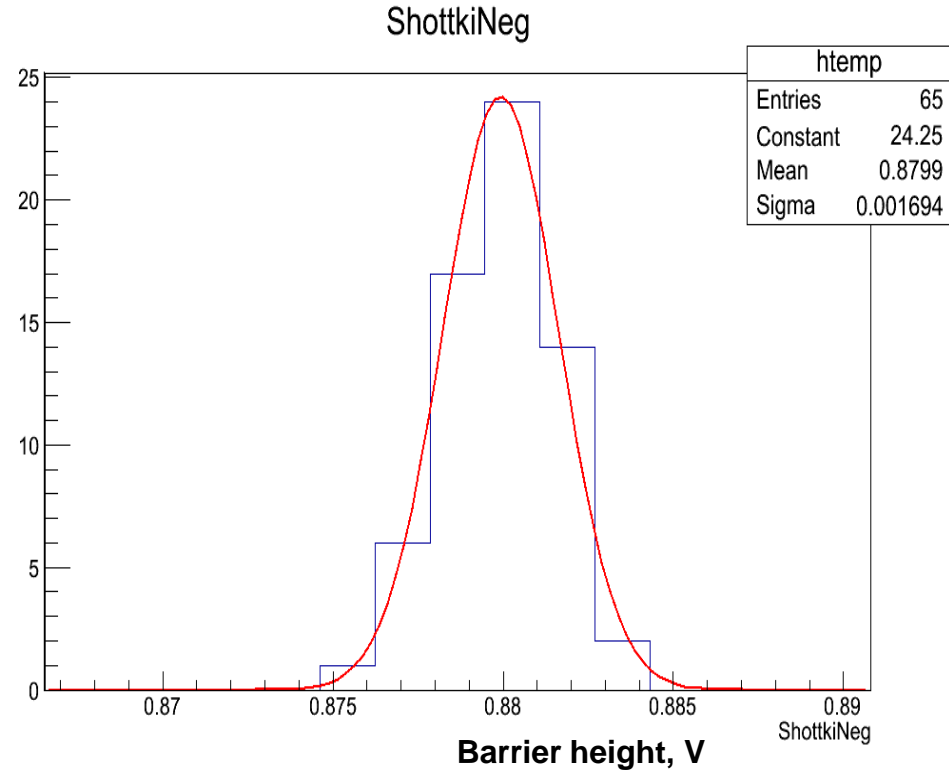
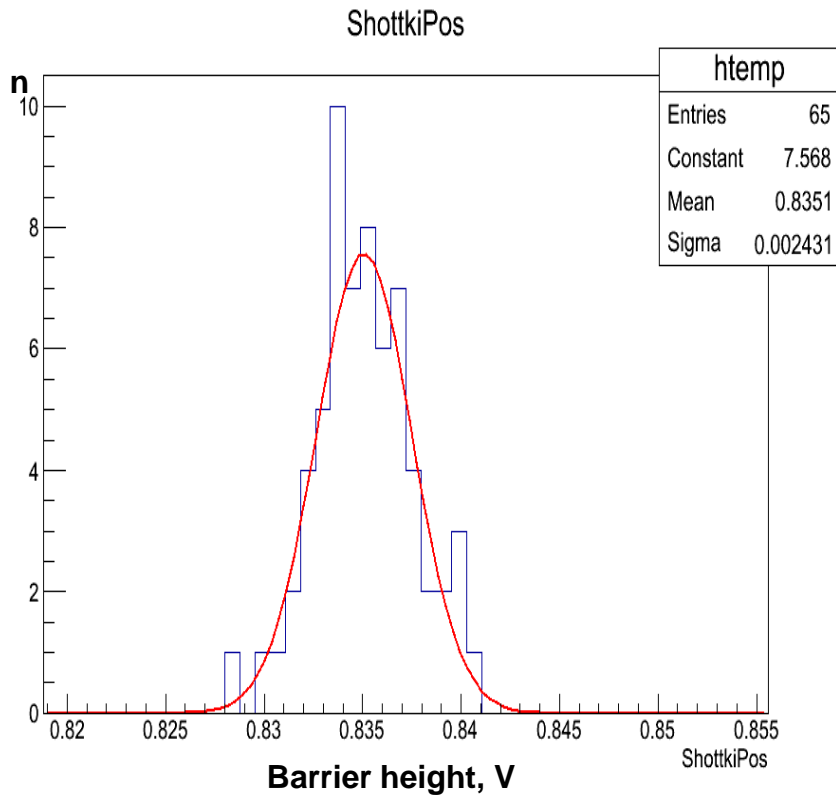
$$I_n = SA_n^* T^2 \exp\left(-\frac{q\varphi_{Bn}}{kT}\right) \quad [1]$$

S - Cross-sectional area, $A_n^* = 8.16 \text{ A} \cdot \text{cm}^{-2} \cdot \text{K}^{-2}$ - Richardson constant for GaAs

T - Temperature of device, q - electron charge, k - Boltzmann constant

φ_{Bn} - barrier height on border of metal–*semiinsulating* gallium arsenide

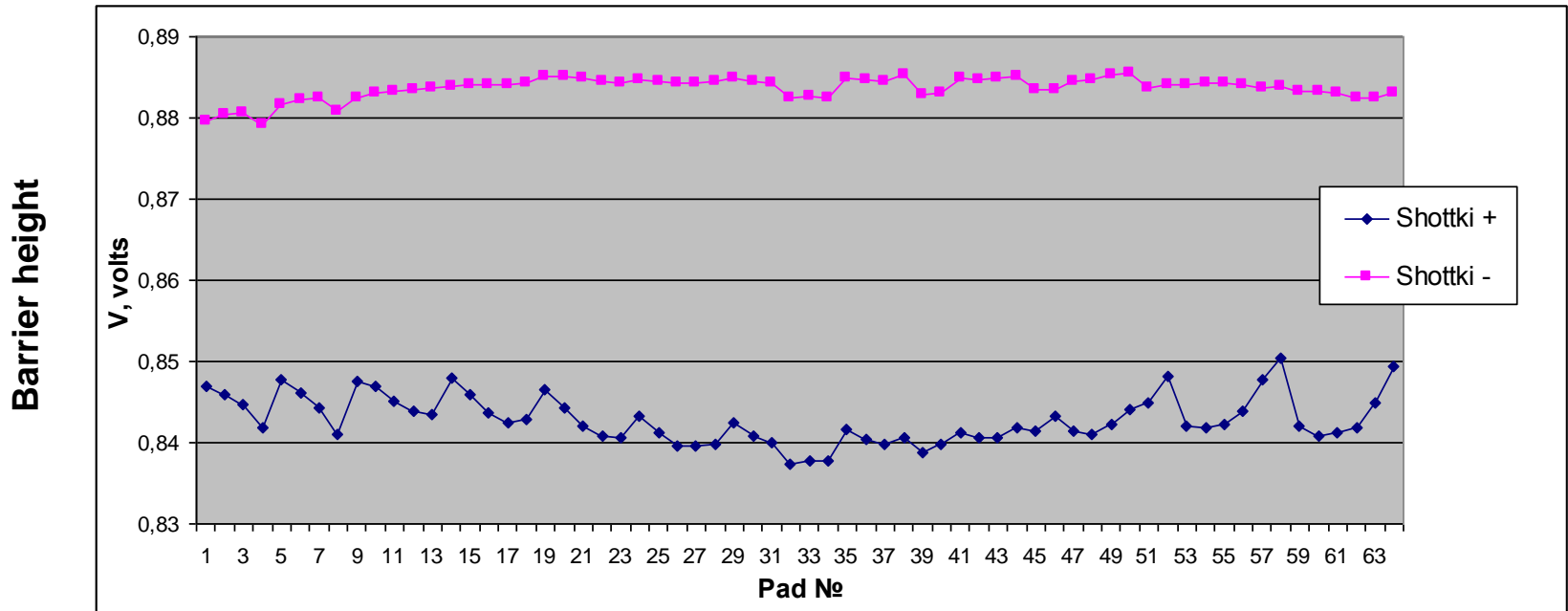
Shottky barrier height distribution of AG221N06



The Schottky barrier height is measured for both polarities. Positive branch corresponds to the barrier on the border Pad-GaAs, negative corresponds to the barrier on the border Backplane-GaAs.

Previously measured and published value for contact based on vanadium **$0.81 \pm 0.02V$** [1]

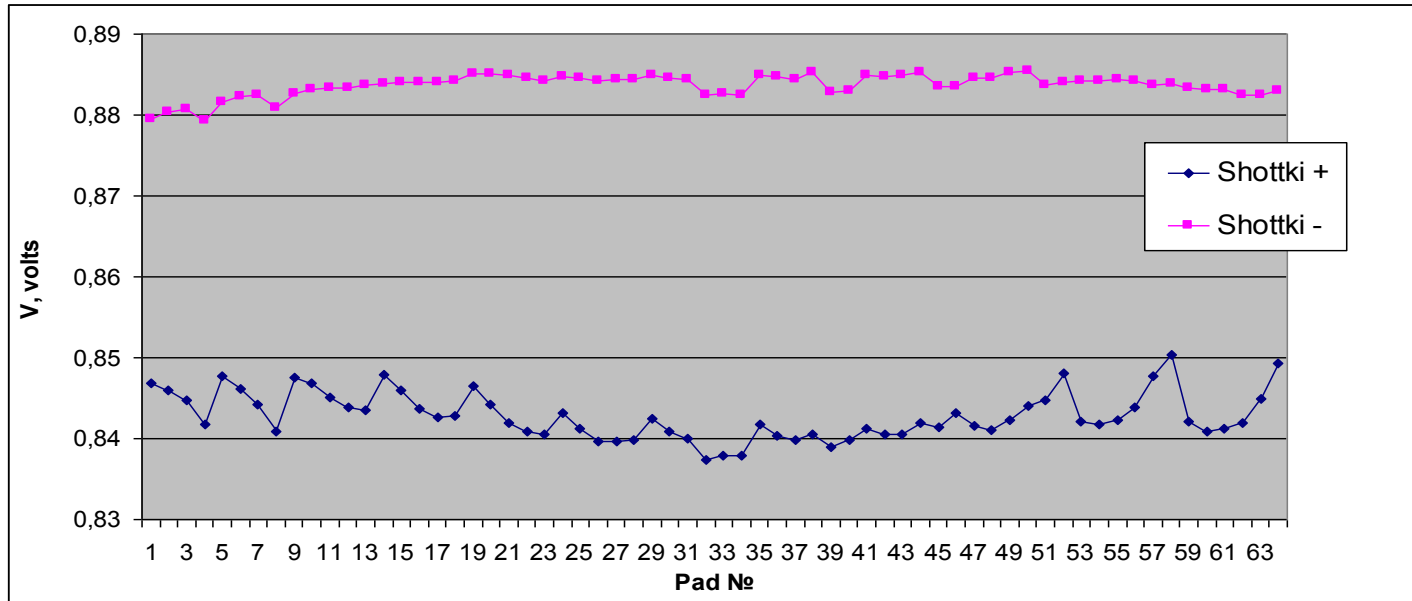
Barrier height distribution of AG221N_o6



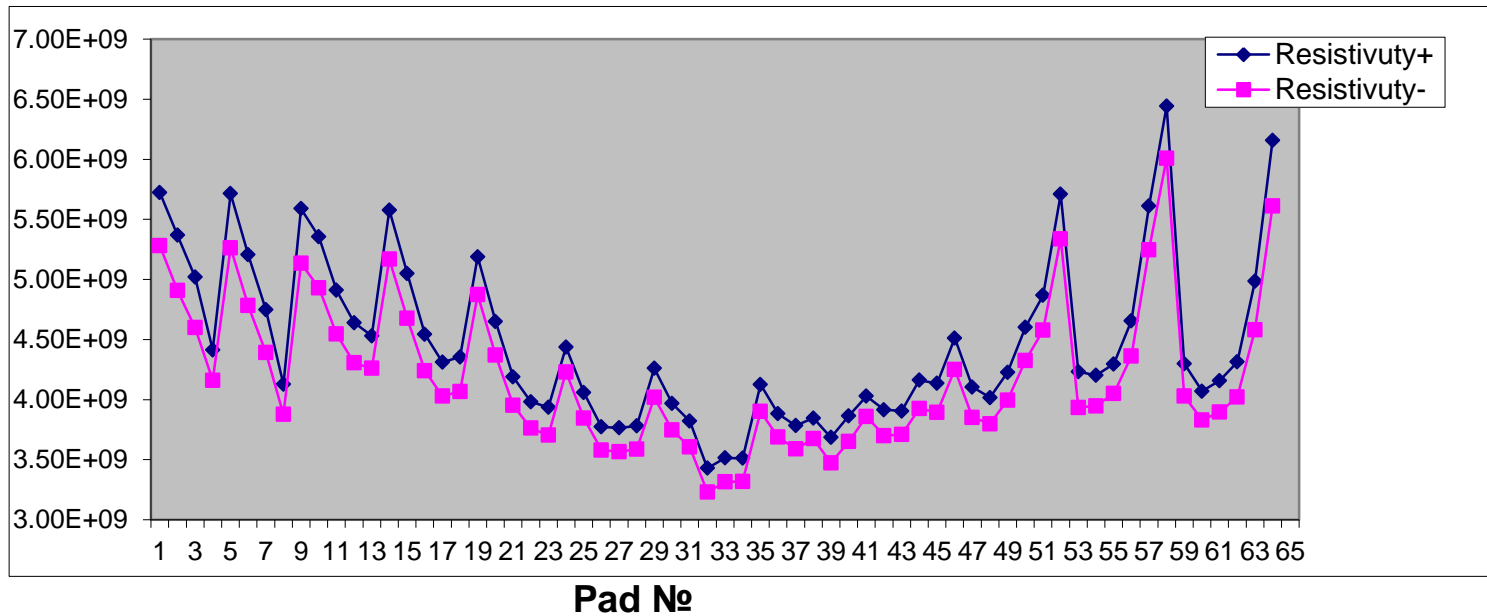
The sensors with ρ^+ , ρ^- dependence on Ring No have similar behavior for ψ^+ , but not for ψ^-

Barrier height distribution of AG221№6

Barrier height



Resistivity, Ω



Average resistivity and barrier height of 11 sensors

№	Detector	Thickness, um	Resistivity, Ohm*cm		Barrier height, volts	
			ρ^+	ρ^-	φ^+	φ^-
1	AG-262 №1	506	3,27E+009	3,05E+009	0,835	0,880
2	AG-262 №3	512	3,10E+009	2,90E+009	0,835	0,880
3	AG-262 №4	509	3,25E+009	3,09E+009	0,837	0,884
4	AG-221 №6	498	4,47E+009	4,19E+009	0,843	0,884
5	AG-262 №12	504	3,38E+009	3,26E+009	0,838	0,884
6	AG-262 №13	517	2,72E+009	2,58E+009	0,833	0,883
7	AG-262 №15	518	3,22E+009	3,06E+009	0,837	0,884
8	AG-262 №16	509	3,63E+009	3,49E+009	0,839	0,885
9	AG-262 №19	507	3,25E+009	3,08E+009	0,836	0,884
10	AG 84 № 23	492	2,92E+009	2,78E+009	0,833	0,880
11	AG 84 №24	485	3,08E+009	2,93E+009	0,834	0,881
Average ± Sigma			3,30±0,45 E+09	3,13±0,43 E+09	0,836±0,003	0,883±0,002

Defects found

The criteria for a pad accepted as good:

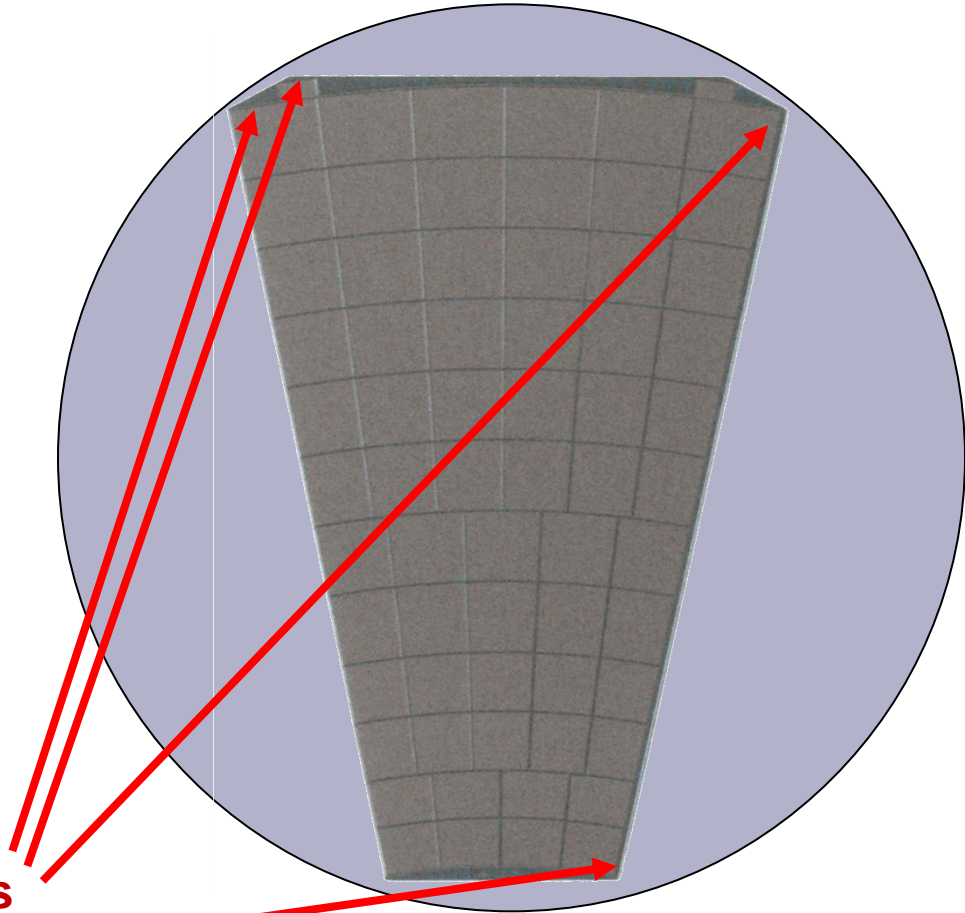
$$\rho > 10e9 \Omega \cdot \text{cm}$$

Some pads or guard rings have untypical behavior.

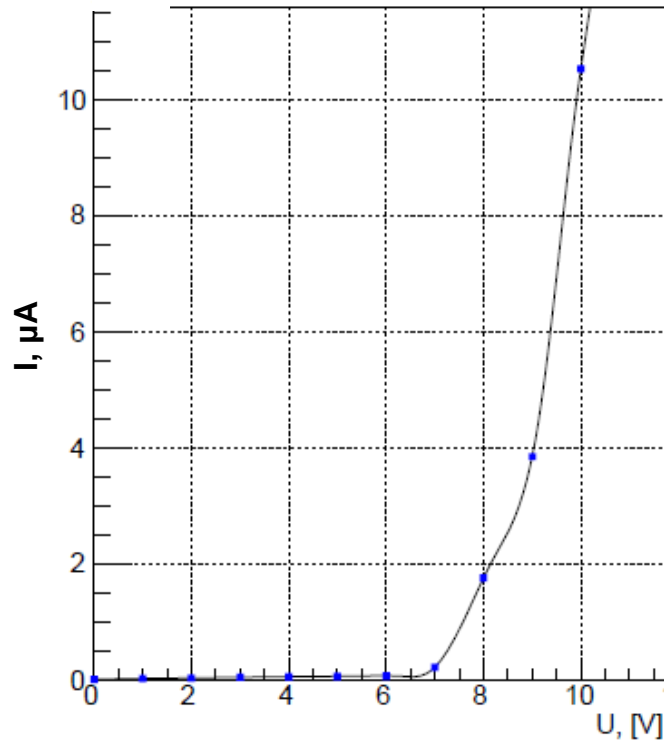
8 of 22 sensors have deflection
Guard ring and one pad:
that may be related
internal structure injury. It
appear on the crystal
boundary for all cases.

All 8 sensors are made of the
same crystal AG84!

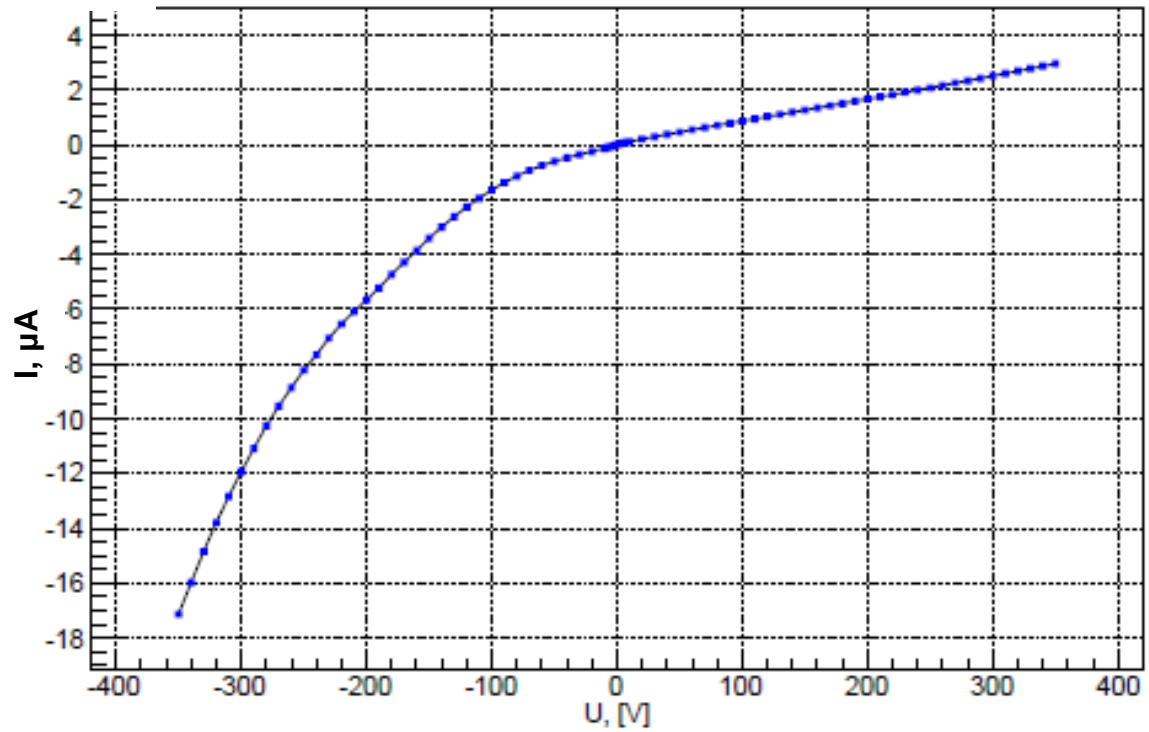
Unusual pads
Guard ring +
Ring1-Pad4; Ring12-Pad1; Ring12-Pad6;



Unypical IV behavior



Ag84N24 Guard ring

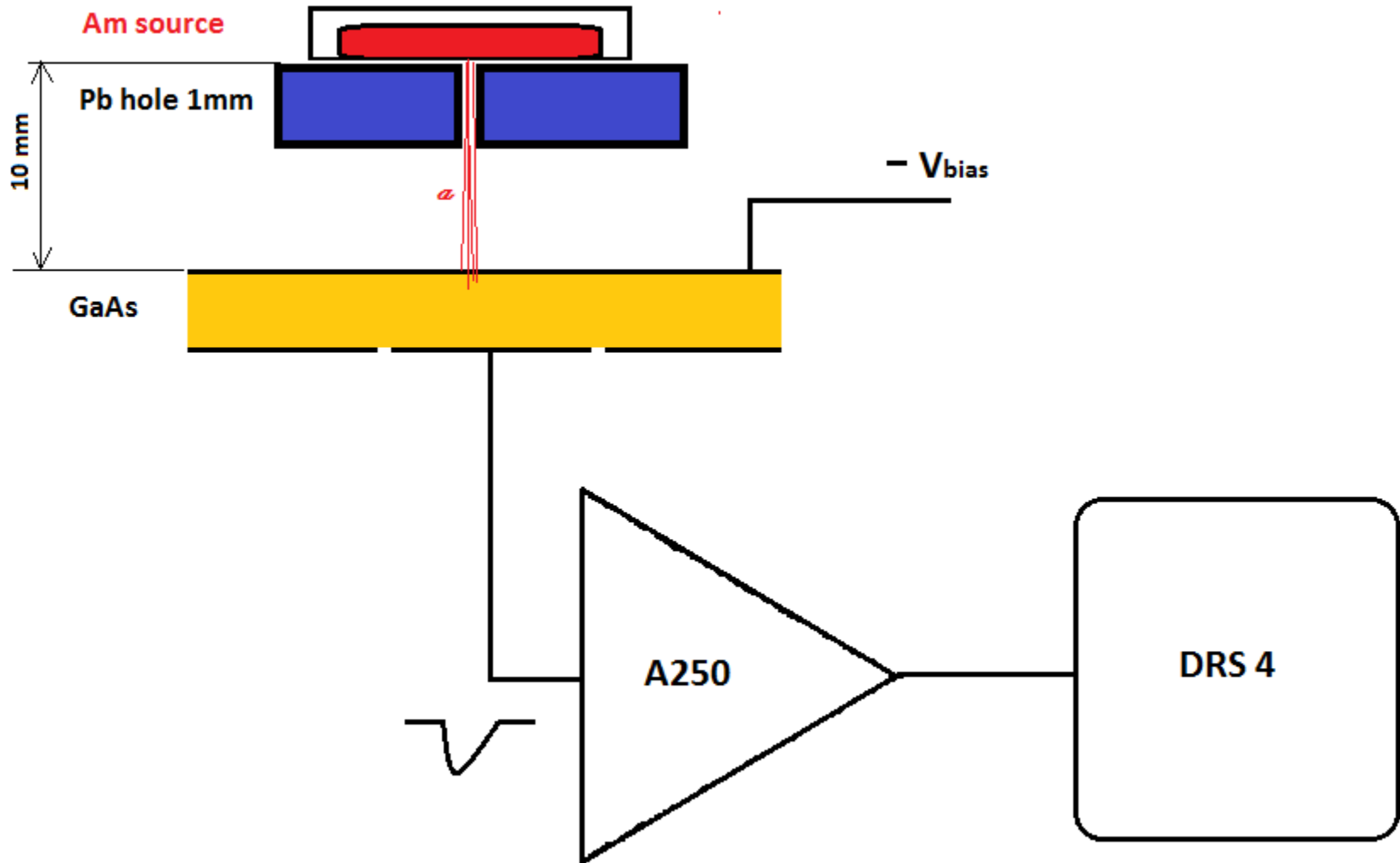


Ag84N23 Ring 1 Pad 4

8 of 22 planes have 1 unusual pad and GR (All 8 of 12 € AG84)

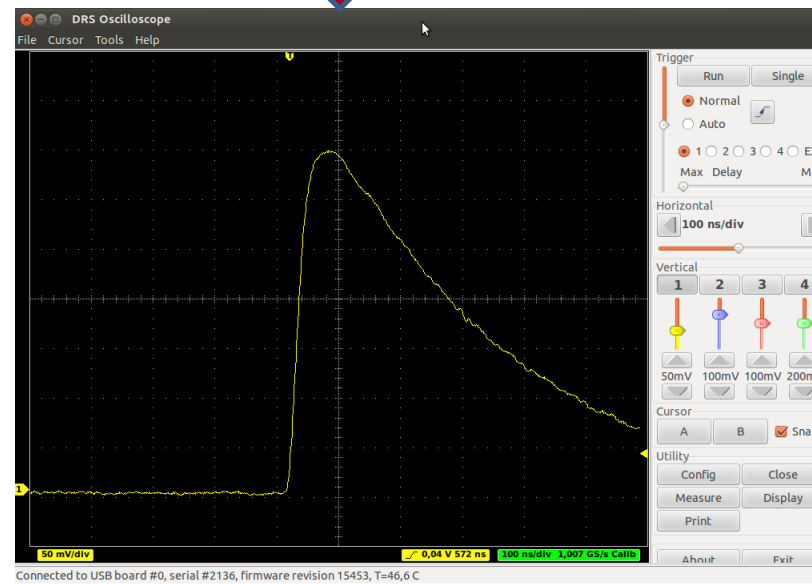
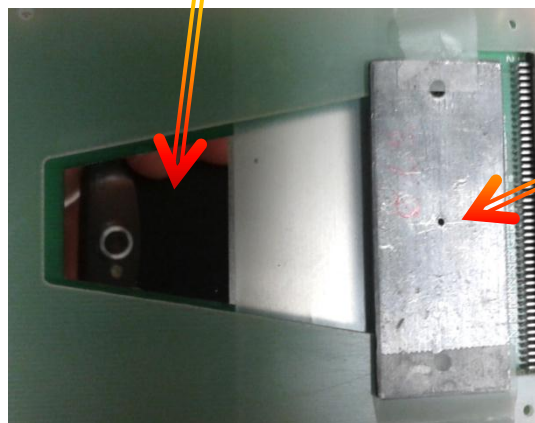
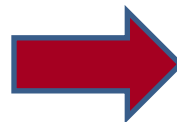
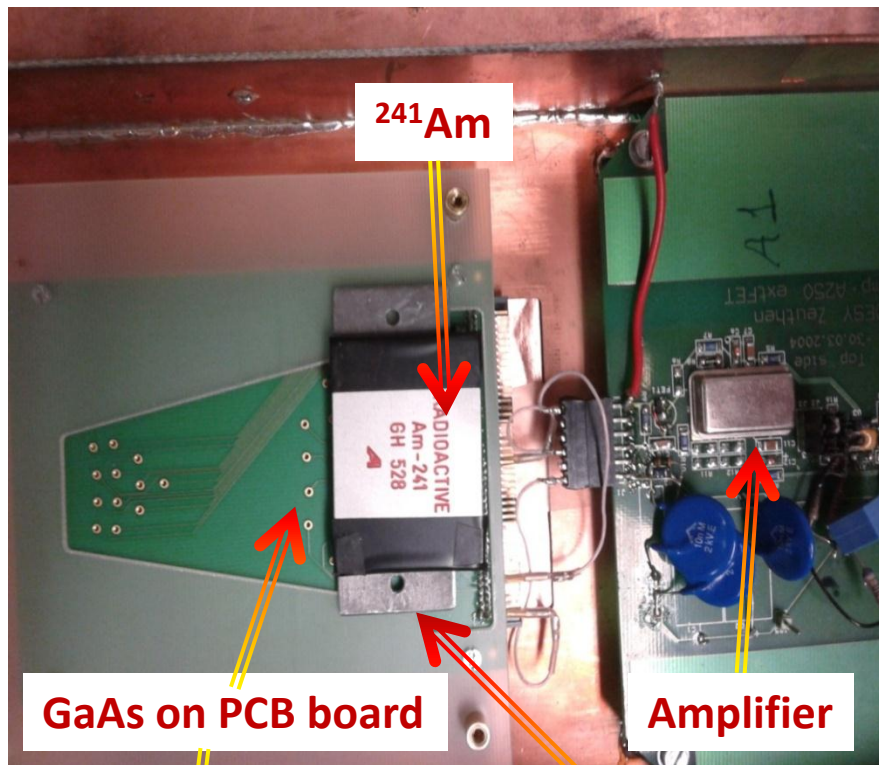
N°	Pad N°	Breakdown voltage, V
AsGa84N7	Guard ring	-330
AsGa84N7	Ring12-Pad1	-310
AsGa84N13	Guard ring	-160; +200
AsGa84N13	Ring12-Pad6	-280
AsGa84N21	Guard ring	+30
AsGa84N21	Ring1-Pad4	+50
AsGa84N26	Guard ring	-110; +230
AsGa84N26	Ring12-Pad1	-210
AsGa84N28	Guard ring	-300
AsGa84N28	Ring12-Pad6	+330
AsGa84N41	Guard ring	+110
AsGa84N41	Ring12-Pad6	+110
AsGa84N23	Guard ring	$\rho < 1E08$
AsGa84N23	Ring1-Pad4	$\rho < 1E08$
AsGa84N24	Guard ring	+10
AsGa84N24	Ring1-Pad4	+10
AsGa84N24	Ring12-Pad6	+30

α -spectra ^{241}Am experimental setup.

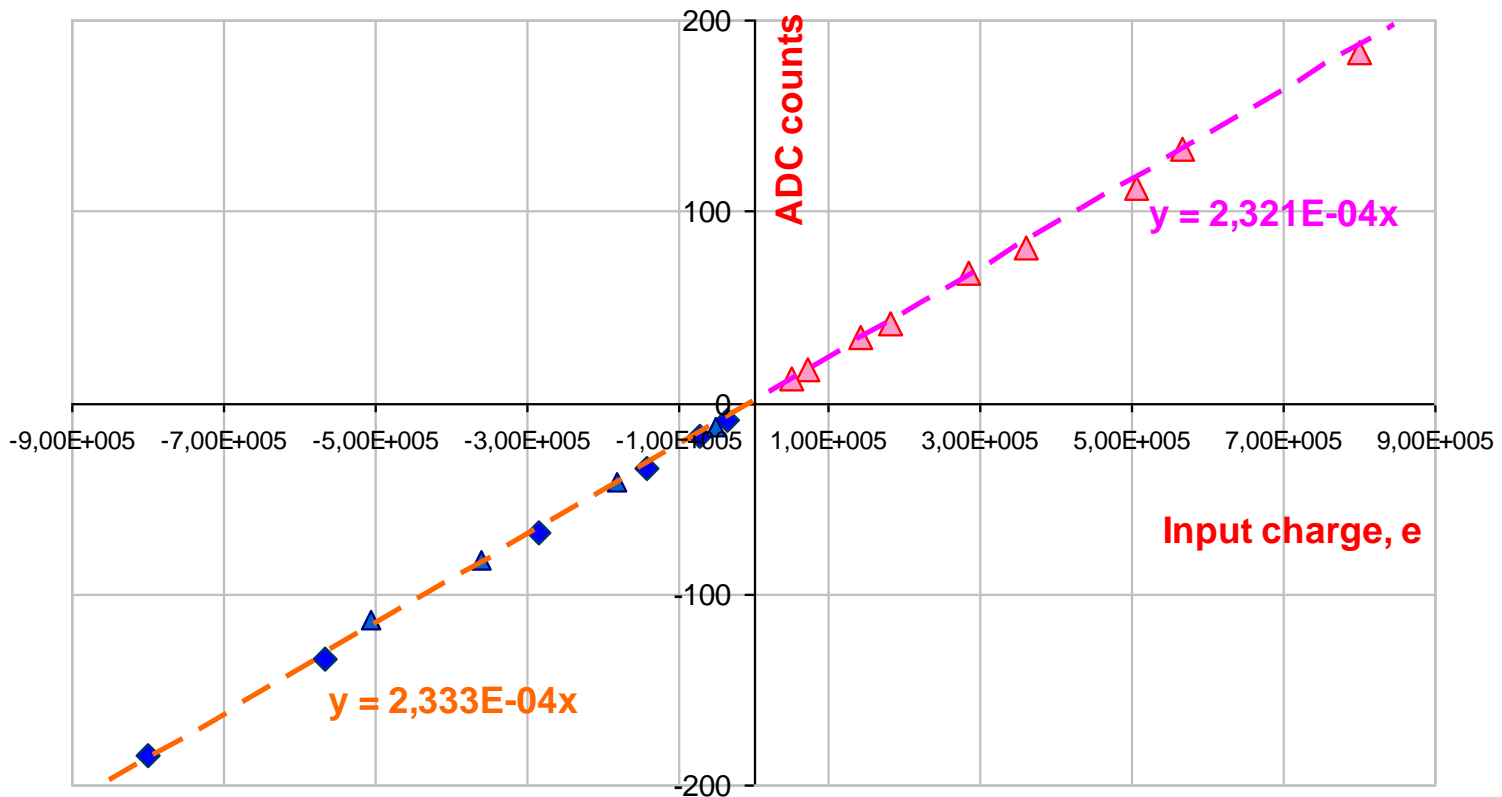


Sensor **AG84N13** has several bonded pads, Ring 12 Pad 3 was connected for measurement.

α -spectra of ^{241}Am experimental setup.



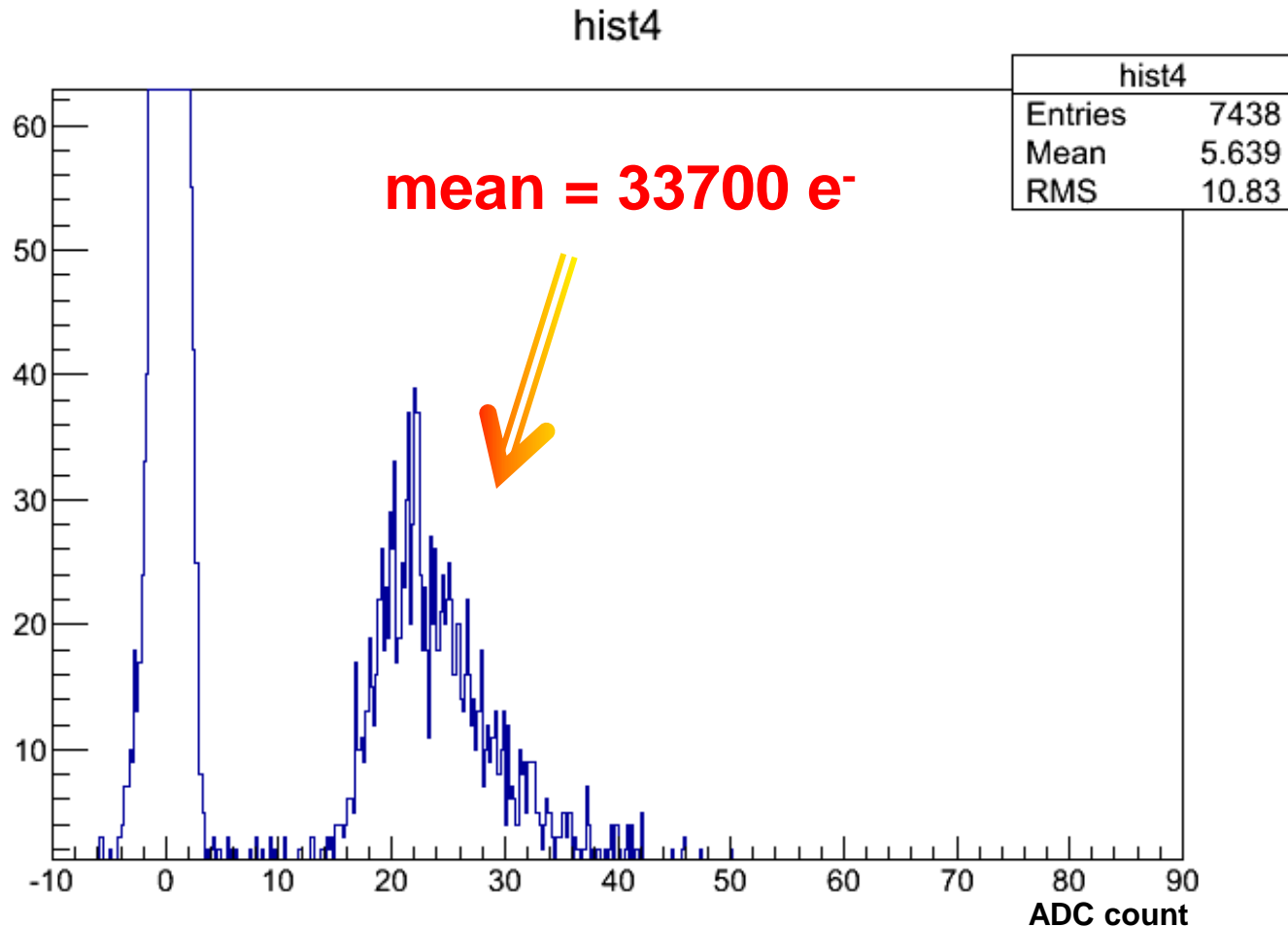
Amplifier & readout calibration.



For both positive and negative signal polarity calibration gives same value:

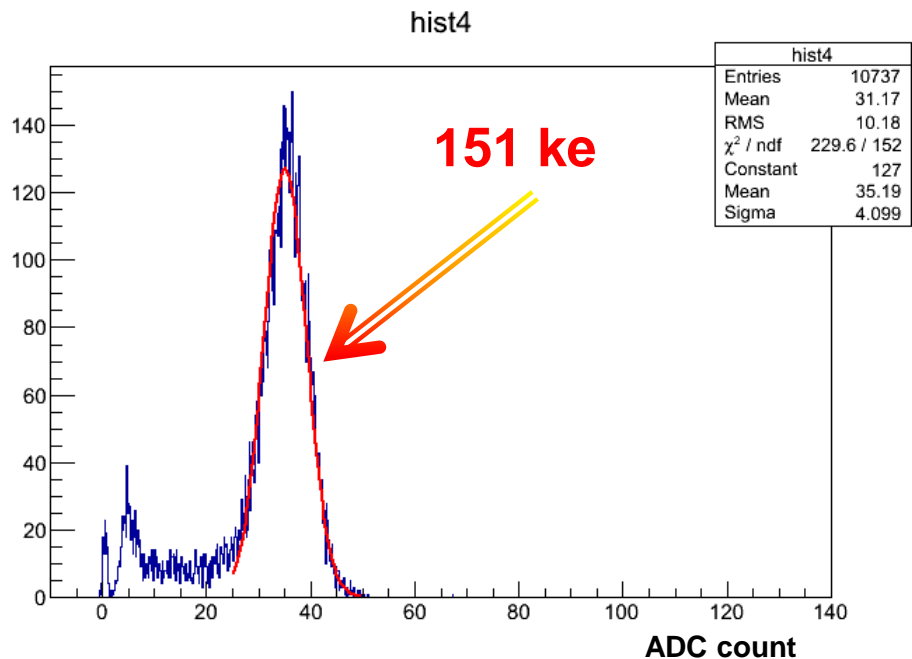
$$1\text{count} = 4,29E03 e^-$$

MIP -spectrum of ^{90}Sr

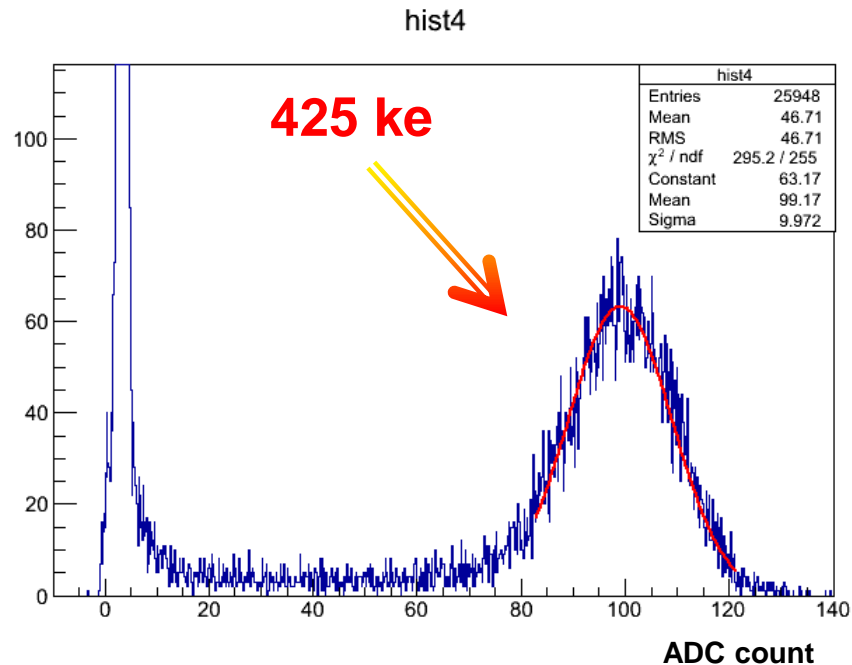


**Sr MIP measured with $V_{\text{bias}} = -400\text{V}$ gives the signal 33700
MIP produces ~ 150 e/h pairs per $1\mu\text{m}$,
it corresponds CCE $\sim 45\%$ or 90% for electron collection
only.**

α -spectra of ^{241}Am



Vbias = -50V



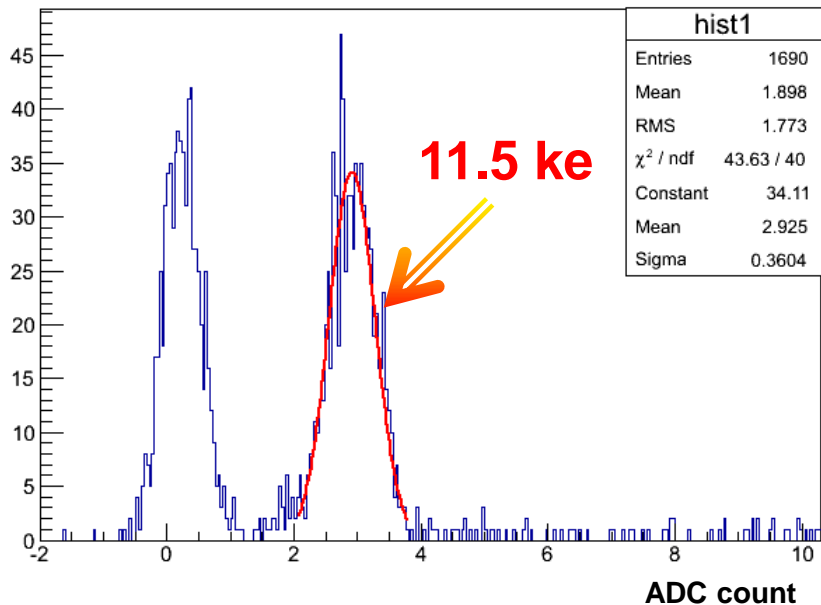
Vbias = -300V

Am from BP, $V_{\text{th}} = 10\text{mV}$, Gauss fit.

Signal from α is rising with V_{bias} , but Signal/Sigma rate is not so critical: 8.8 for -50V, 9.9 for -300V.

α -spectra of ^{241}Am

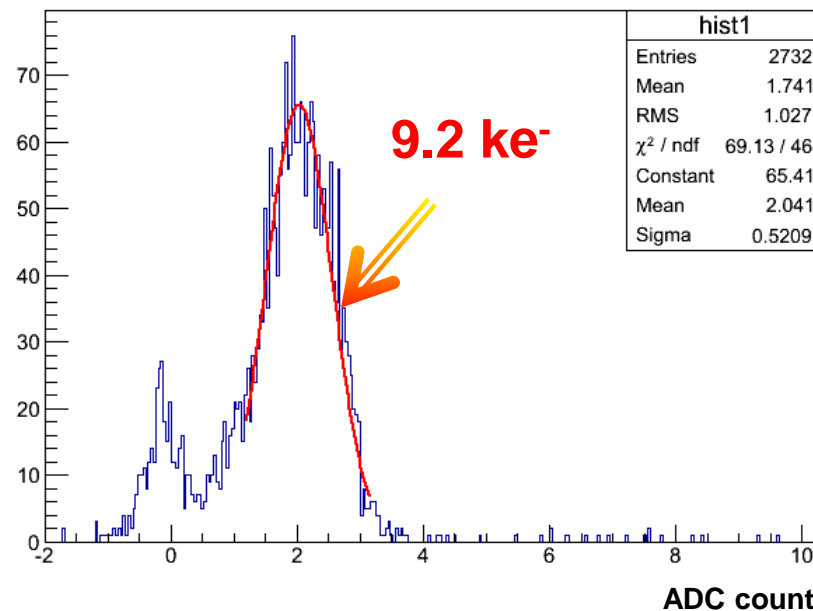
hist1



Vbias = -400V

Am source closed by the 50 μm Cu foil to kill alpha. All big signals escaped and rate dropped from 300Hz to \sim 2Hz. About 12ke signal may be part of Am 60keV.

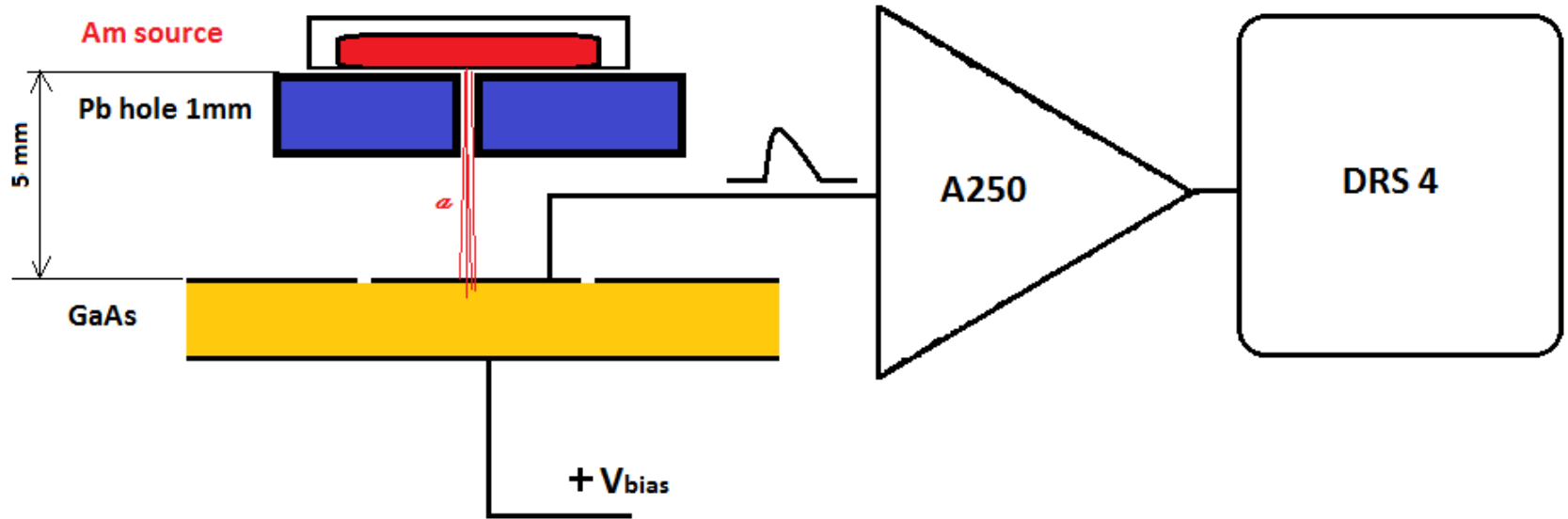
hist1



Vbias = +300V

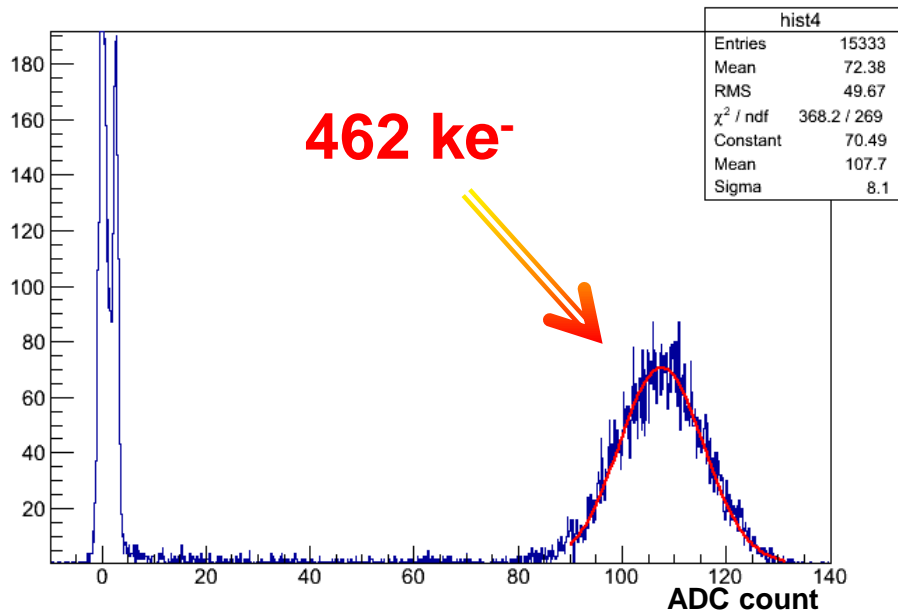
Reversing Vbias = +300V gives only 9.8 ke signal mean and rate dropped from 300Hz to \sim 6 Hz. It proves only electron charge collection for GaAs:Cr.

α -spectra of ^{241}Am from Pad.



α -spectra of ^{241}Am

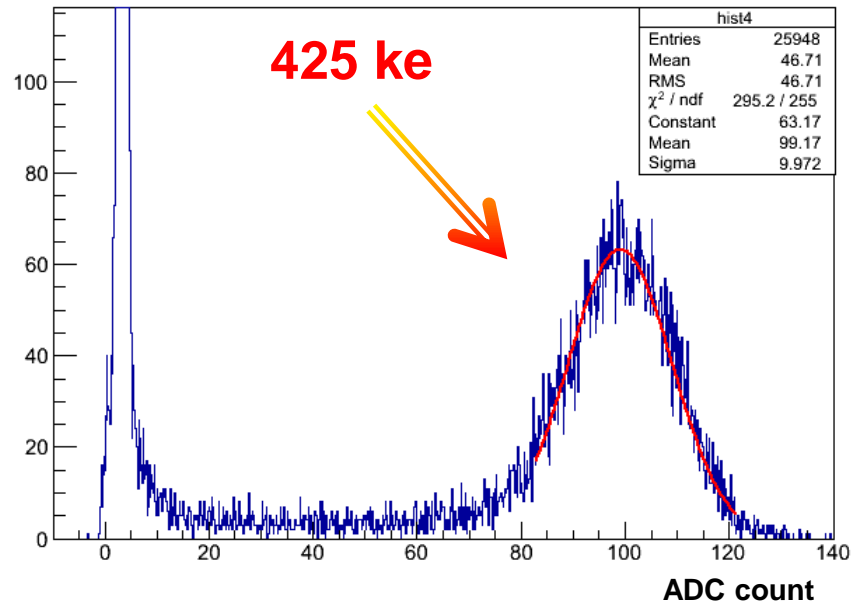
hist4



Vbias = +300V

Am from Pad

hist4



Vbias = -300V

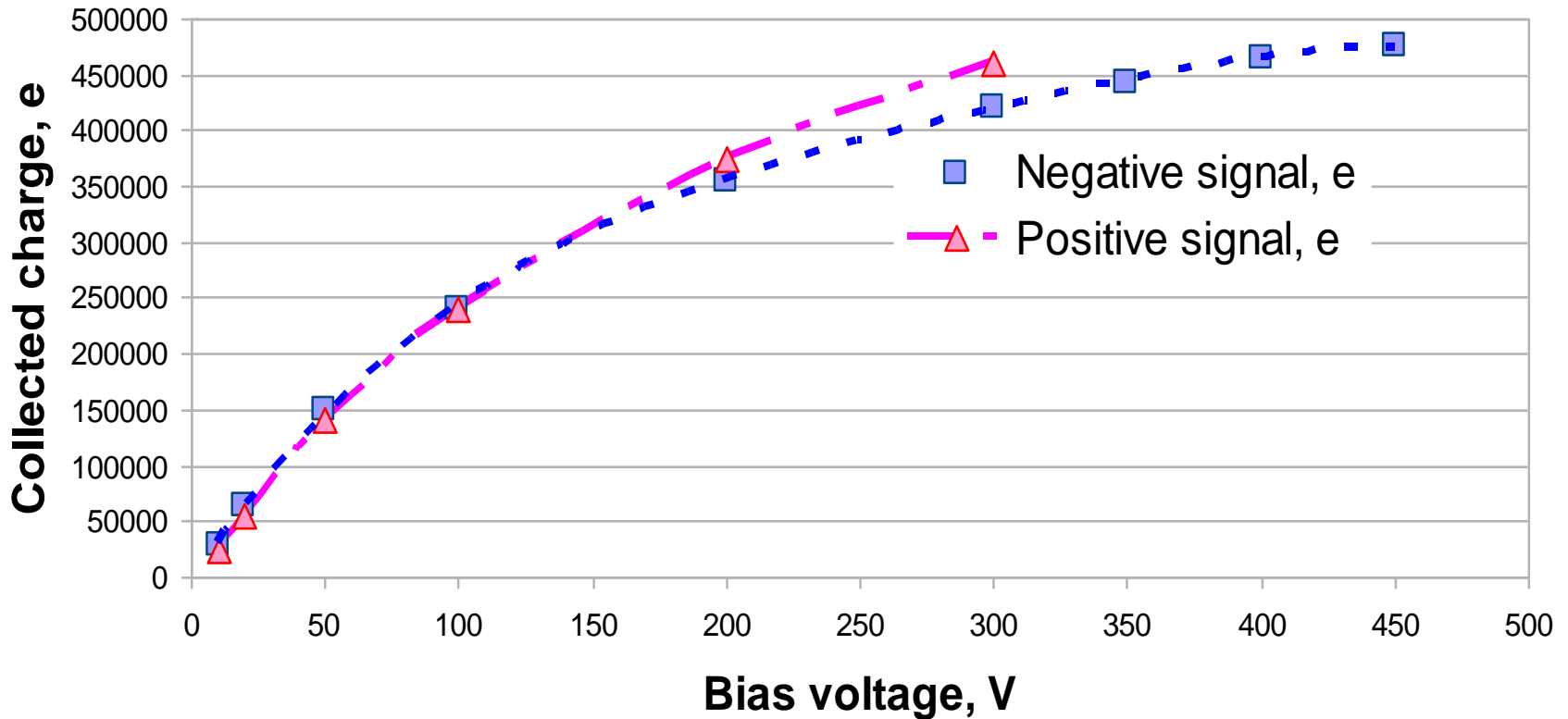
Am from BP

When α comes from pad, the signal a bit higher (8% for $V_{\text{bias}}=300\text{V}$),
Also signal/noise ratio is better : 13 vs 10.

This can be explained by the fact that the distance from the source to the pad
was in the first case 5mm, the second 10 mm.

α -spectra of ^{241}Am charge collection vs V_{bias}

AG84N13 Ring 12 Pad 3



Charge collection was measured at different V_{bias} up to 1V/ μm . There is a tendency to saturation.

For the positive V_{bias} is limited to 310V due to noise.

Summary

DESY's experimental set-up has been applied for measurement of I/V and temperature dependence of GaAs sector sensors (I-V, ρ , ϕ_{Bn})

The results are:

- ✓ I-V of 11 new sensors was measured
- ✓ I-V behavior is well consistent with previous results and theoretical calculations.
- ✓ The resistivity and the barrier height on the border metal-semiinsulating GaAs was measured for all pads.
- ✓ Together with previous measurements now all 22 sector size sensors are certified:
 - 14 were recognized as completely good,
for all pad $\rho > 10e9 \text{ GOhm} \cdot \text{cm}$, $0.8\text{V} < \phi_{Bn} < 0.9 \text{ V}$.
 - 7 has defects the current exceed the limit for one polarity in Guard ring and one pad. 1 sensor has GR resistivity $\sim 10e08$ for negative polarity.
- ✓ α -spectra of ^{241}Am were measured for different Bias voltages, polarity, geometry.
- ✓ only electron charge collection approved.
- ✓ collected charge slightly depends on the bias voltage polarity, but strongly depends on its value and the interaction depth in the detector.

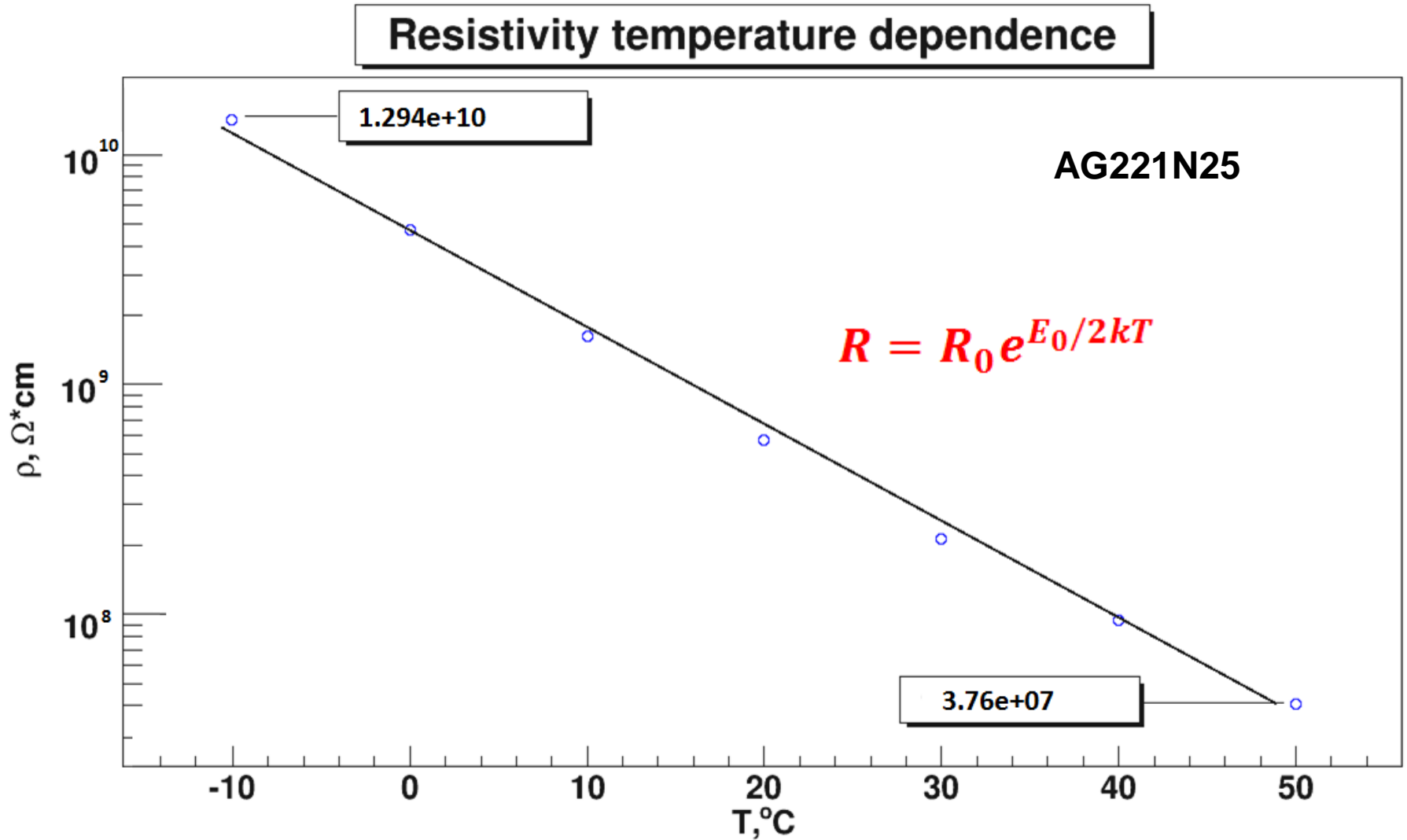
We have all 22 sensors tested.

References

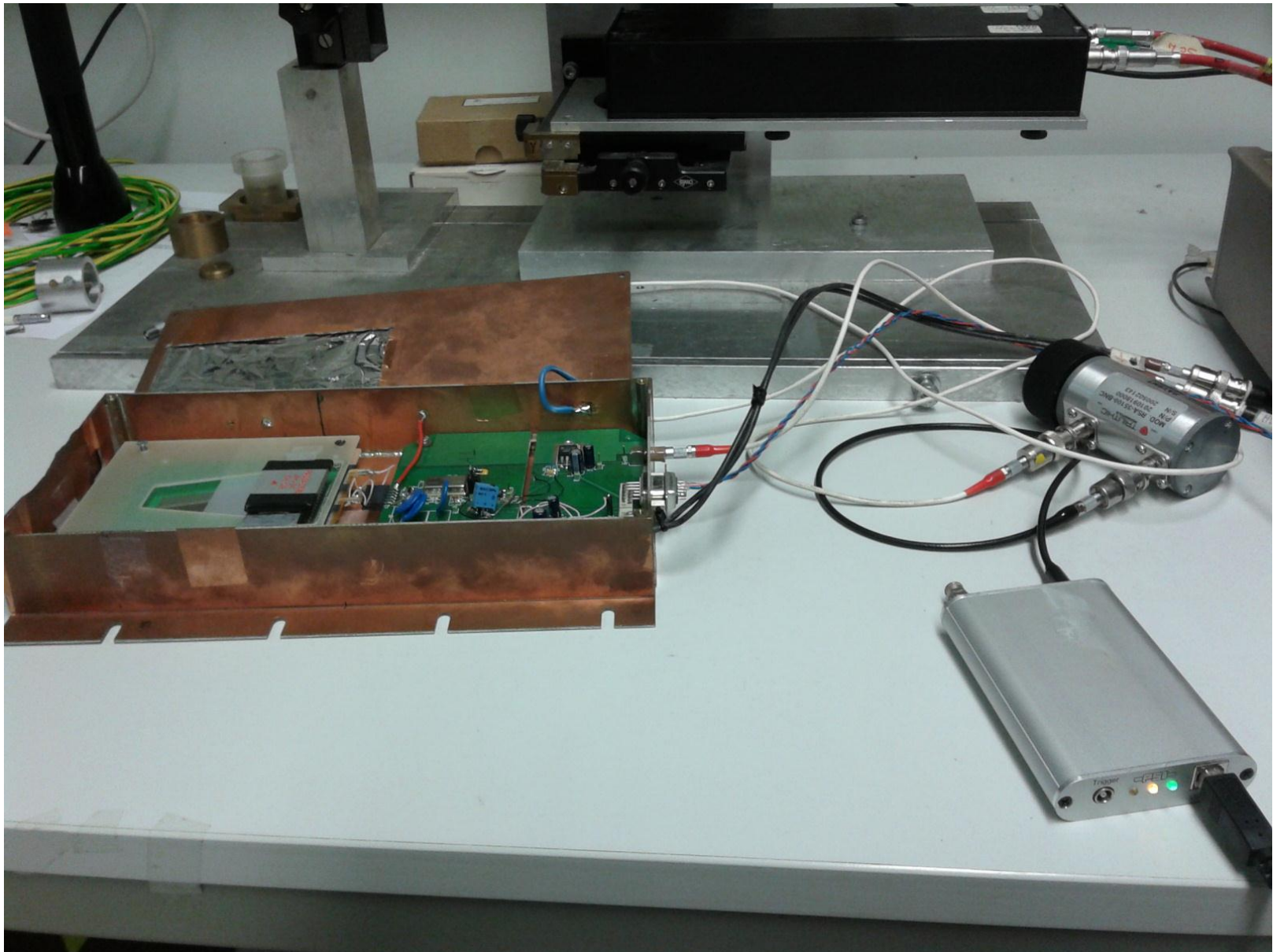
- 1. Measurement of the barrier height on border of metal–semiinsulating gallium arsenide.** *G.I. Ayzenshtat, M.A. Lelekov, O.P. Tolbanov. Физика и техника полупроводников , 2007, том 41, вып. 11*
- 2. Current transport in gallium arsenide detector compensated by chromium**
G.I. Ayzenshtat, M.A. Lelekov, V.A. Novikov, L.S. Okaevitch, O.P. Tolbanov. Физика и техника полупроводников , 2007, том 41, вып.5

Backup slides

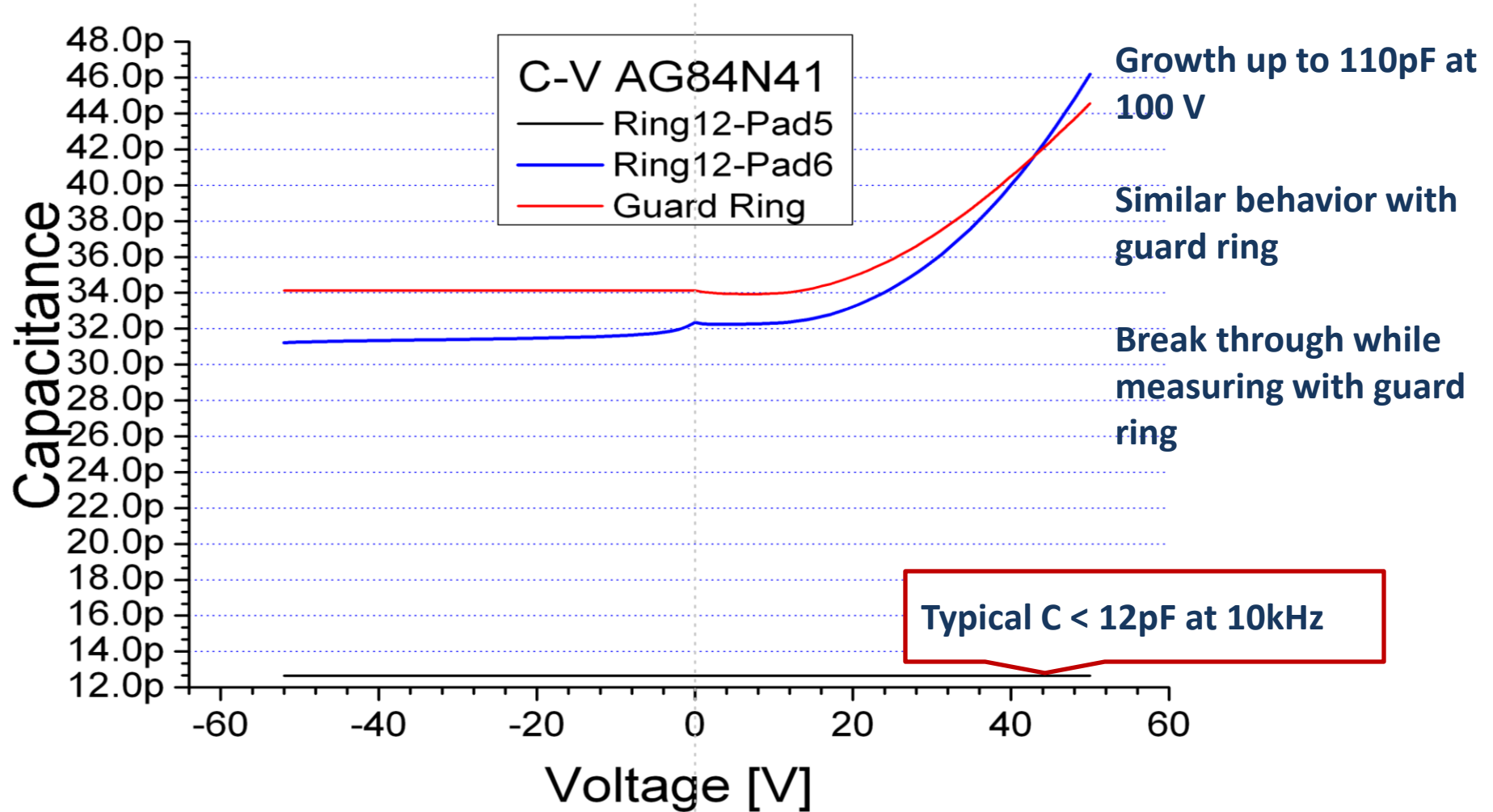
Temperature dependence of the resistivity



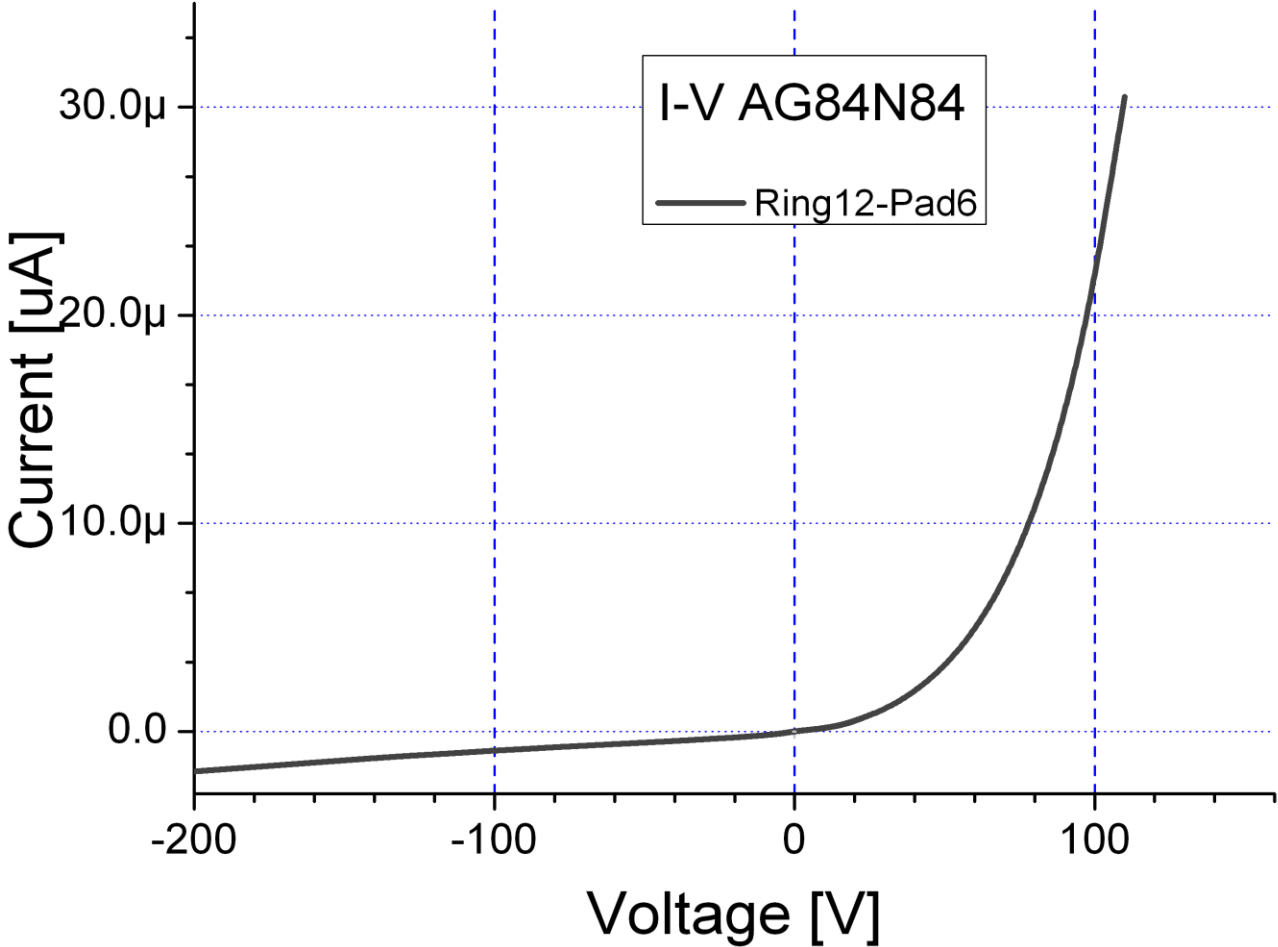
α -spectra of ^{241}Am experimental setup.



Unusual pad, unusual guardring and normal pad C-V



Unusual pad I-V



Growth up for positive Vbias

Normal behavior in negative area

Similar behavior with guard ring

Average resistivity and barrier height of 11 sensors

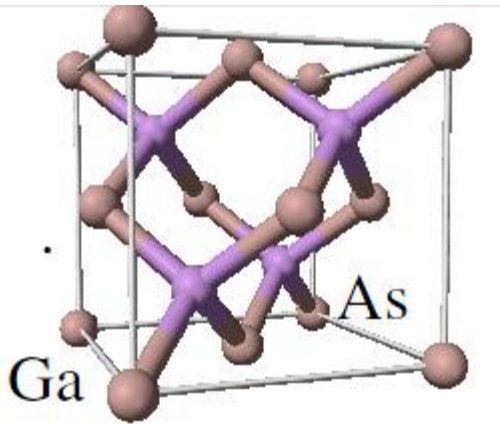
№	Detector	thickness, um	Resistivity, Ohm*cm		DARRIER height, volts	
			ρ^+	ρ^-	ϕ^+	ϕ^-
1	AG-84 №13	498	Not processed	Not processed	Not processed	Not processed
2	AG 84 № 26	502	1.20E9	1.10E9	0.75	0.74
3	AG 84 № 7	490	2.25E9	2.18E9	0.78	0.79
4	AG 84 № 19	495	3.00E9	2.79E9	0.78	0.78
5	AG 84 № 21	492	2.42E9	2.37E9	0.76	0.76
6	AG 84 № 32	502	3.20E9	3.04E9	0.78	0.77
7	AG 84 № 39	495	3.71E9	3.48E9	0.79	0.76
8	AG 84 № 41	487	4.07E9	3.84E9	0.76	0.75
9	AG 84 № 29	487	3.67E9	3.23E9	0.78	0.81
10	AG 84 № 28	500	2.09E9	1.92E9	0.76	0.77
11	AG 221 №25	492	2.49E9	2.42E9	0.79	0.81

Forward region of the ILC

Beam calorimeter (BeamCal) - monitor the beam parameters at the interaction point; adjacent to the beampipe.

Luminosity detector (LumiCal) – covers larger polar angles; luminometer of the detector.

The gamma detector (GamCal) – together with BeamCal, measures beamstrahlung photons, which are very collinear to the beam.



Gallium arsenide (GaAs)

Compound semiconductor, direct bandgap

Two sublattices of face centered cubic lattice
(zinc-blende type)

GaAs grown by Liquid Encapsulated
Czochralski (LEC).
doped by Te or Sn (shallow donor)
to fill EL2+ trapping centers.
Compensated by Cr (deep acceptor) to
high-ohmic intrinsic material.
Compensation is temperature controlled

Semi-insulating - no p-n junction

Signal charge transport mainly by electrons

Structure provided by metallisation (similar to
diamond)

<input type="checkbox"/> Density	5.32 g/cm ³
<input type="checkbox"/> Pair creation E	4.3 eV/pair
<input type="checkbox"/> Band gap	1.42 eV
<input type="checkbox"/> Electron mobility	8500 cm²/Vs
<input type="checkbox"/> Hole mobility	400 cm ² /Vs
<input type="checkbox"/> Dielectric const.	12.85
<input type="checkbox"/> Radiation length	2.3 cm
<input type="checkbox"/> Ave. Edep/100 μm (by 10 MeV e ⁻)	69.7 keV
<input type="checkbox"/> Ave. pairs/100 μm	13000
<input type="checkbox"/> Structure	p-n or insul